



# Comparison of Test Methods for High-Performance Thermal Interface Materials

Authored by: Bob Jarrett and Jordan Ross, Indium Corporation, Jim Hisert and Craig K. Merritt.

## Abstract

This paper compares the application of two methods for testing thermal interface materials to the development and characterization of high performance materials. Particular strengths of different test methods provide a more complete understanding of TIM performance. In combination, the tools provide effective development and improved metrics. The limitations in resolution and repeatability are discussed.

**Keywords:** TIM testing, ASTM D5470, thermal test vehicle

## Thermal Interface Testing

At the 2006 Semi-Therm 22<sup>nd</sup> Conference, Lasance, et al. [1] presented a summary of the challenges facing thermal interface material testing. These challenges include the issues of repeatability and reproducibility of any test method as well as the applicability of the tests to behavior of the TIM in service. These issues continue to rise as a wider variety of TIM materials are introduced into the market for the ever-increasing heat load demands on the thermal solutions.

Thermal resistance tests include steady state methods such as prescribed in the ASTM D5470 standard [2] and various types of thermal test vehicles [3, 4], and transient methods such as the electrical temperature measurement [5] and the laser flash test [6].

In this paper, we limit our discussion to experiences with variations of the steady state test method. Details of the equipment are described elsewhere [3, 7]. We review

experiences with evaluating and developing high-performance TIM materials and the correlation of the different testing methods. These evaluations include some data from initial installed material, as well as the performance resulting from exposure.

## Steady State Testing Configurations

Figures 1 and 2 are schematics of the two steady state test methods used. The ASTM D5470 test stand consists of a press to apply the clamping force to the interface between the heat source and the heat-sink. The instrumentation includes a load cell for the pressure, a precision power supply to drive the resistive heaters, a temperature-controlled circulating fluid for the cooling block, and temperature sensors embedded in metering blocks attached to the heat source and sink. The temperature sensors are 4-wire resistive temperature devices (RTDs).

## BOB JARRETT



**Bob Jarrett**, Process Engineer/Metallurgist/Thermal Engineer for Indium Corporation, supporting Indium Corporation's Specialty Metals Division. He focuses on process metallurgy in the casting, extrusion, and rolling operations.

Bob founded Indium Corporation's Thermal Lab and developed the test methods for supporting Indium's thermal products. He is co-inventor of the patented Heat-Spring<sup>®</sup> and mdTIM technologies, and he serves as the technical support for thermal and heat transfer issues. Bob has authored several papers and presentations on thermal interface materials.

Bob is a Six Sigma Brown Belt from the Thayer School of Engineering at Dartmouth College. He serves as an Adjunct Professor of Materials Science at SUNY Polytechnic Institute in Marcy, NY.

**email:** [bjarrett@indium.com](mailto:bjarrett@indium.com)

**Full biography:**

[www.indium.com/biographies](http://www.indium.com/biographies)

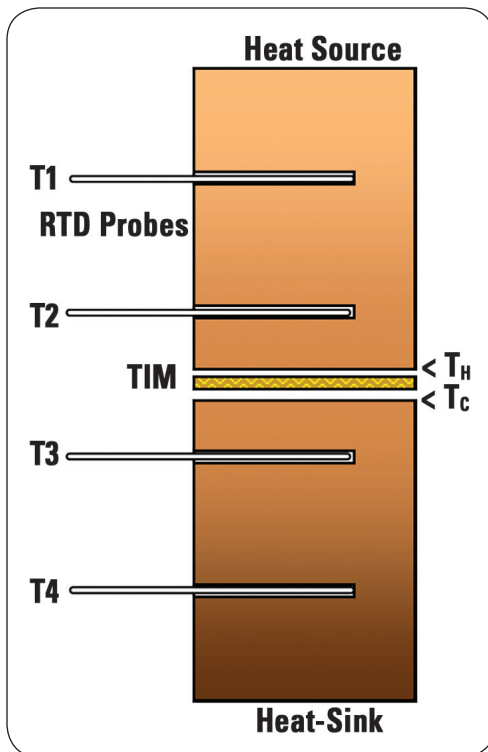


Figure 1. Schematic of TIM and test block configuration of ASTM D5470 tester.

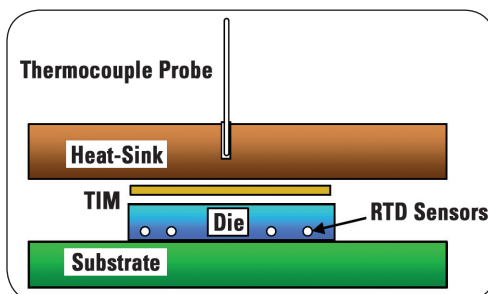


Figure 2. Schematic of TIM thermal test vehicle.

With the assumption of linearity, two RTDs in a fixed geometry in the blocks monitor the temperature gradient,  $\Delta T/L$ , in the blocks. This gradient multiplied by the (known) thermal conductivity,  $\lambda$ , of the block determines the heat flow per unit area,  $Q/A$ . Extrapolation of the temperature gradient to the interface surface of the blocks provides the surface temperatures of the TIM material,  $T_C$  and  $T_H$ . With the information about the heat flow and the temperatures of the surfaces of the TIM, the thermal resistance,  $\theta$ , is calculated as  $\theta = (T_H - T_C) \times A/Q$ .

In the thermal test vehicle, a similar methodology is used. An electrically heated IC is instrumented with integral four-wire RTDs. The TIM is applied between the IC surface and a cooling plate held in place by a spring-loaded clamping force. The plate is cooled by symmetric fan-cooled heat-sinks. The cooling plate is instrumented with an embedded thermocouple located above the IC. Since the gradients to the TIM surfaces are not directly measured, each TTV design is calibrated with a factor that includes the thermal resistance contribution of the thickness of the silicon die and the copper between the TIM and the thermocouple.

While the thermal test vehicle has limits in absolute accuracy when measuring thermal resistance, the design closely models the environment a TIM would experience in service. This allows for relevant comparisons of TIM performance of widely different physical characteristics. Together with a standardized test, the TTV lends itself to development and characterization of materials.

## Uncertainty of Measurement

The theoretical uncertainty,  $U^0$ , for the tester is a function of the tolerances in the geometry of test blocks, the thermal conductivity of the calorimeter blocks, and the uncertainties in the temperature measurement. The dimensions of the blocks and the drilled hole locations are measured to within  $\pm 5\mu\text{m}$  and  $\pm 25\mu\text{m}$ , respectively. The thermal conductivity of the blocks is reported in the range of 150–155 W/mK.

For the temperature measurements, the instrument uncertainty is  $0.013^\circ\text{C}$  with a resolution of  $0.001^\circ\text{C}$ . For the different measurements, the upper bound of the uncertainty is  $0.018^\circ\text{C}$ . Internal calibration of the RTDs demonstrated repeatability of the four RTDs to be  $\pm 0.004^\circ\text{C}$ .

## JORDAN ROSS



**Jordan Ross**, Senior Manager for Manufacturing Operations, manages strategic projects and is currently the acting plant manager. He works closely with marketing, maintenance, operations, and engineering to manage projects to meet budget and schedules.

Jordan previously worked in Global Product Management and Global Sales Account Management.

Jordan has a bachelor's degree in Business Administration from the State University of New York Institute of Technology.

He is a strong advocate of clean water and wild fish and started a global non-profit initiative called Trout Power® to help protect and preserve wild trout populations in the United States.

email: [jross@indium.com](mailto:jross@indium.com)

Full biography:

[www.indium.com/biographies](http://www.indium.com/biographies)

Following the NIST methodology [8] for the expanded uncertainty of thermal resistance, measurement for this instrument is  $0.0068\text{cm}^2\text{-}^\circ\text{C/W}$  ( $k=2$ ). An initial test of the repeatability for a single sample repeatedly loaded showed a spread with a standard deviation of  $0.0035\text{cm}^2\text{-}^\circ\text{C/W}$ . This is consistent with the calculated uncertainty of measurement. However, when individual samples of the same lot of material were tested, the standard deviation increased to an unacceptable level of  $0.026\text{cm}^2\text{-}^\circ\text{C/W}$ .

A check of the RTD probes revealed that removing and reseating the probes showed as much as a  $0.1^\circ\text{C}$  offset between measurements—far more than the  $\pm 0.013^\circ\text{C}$  confidence interval. The probe contact to the test block appeared less than expected and the insulation on the length of the probe was not adequately isolating the probe stem from convective cooling.

This combination of a steeper temperature gradient at the probe interface to the block and poor thermal contact with the block resulted in a larger stem loss temperature drop than the  $0.01^\circ\text{C}$  calculated for a probe interface resistance of  $0.5\text{cm}^2\text{-}^\circ\text{C/W}$ .

The contact grease on the RTD probes was removed and replaced with higher performance thermal grease and the insulation was modified to improve its uniformity. With these modifications, the variability of the set-up was reduced to a standard deviation of  $0.008\text{cm}^2\text{-}^\circ\text{C/W}$ .

The stem loss effect on the TTV measurements is less complex. A lowering of the temperature of the  $T_c$  probe offsets the thermal resistance measured to the plate. The temperature difference from the junction to ambient ( $T_j\text{-}a$ ) serves as an indicator for a problem with the thermocouple stem loss. The same adjustments to the TTV probe are incorporated for consistency.

## Results

Figure 3 shows a typical presentation of the data from the ASTM tester. In this evaluation, two types of thermal grease are compared to the response of metallic TIM material. These materials have widely varying response to the applied clamping force.

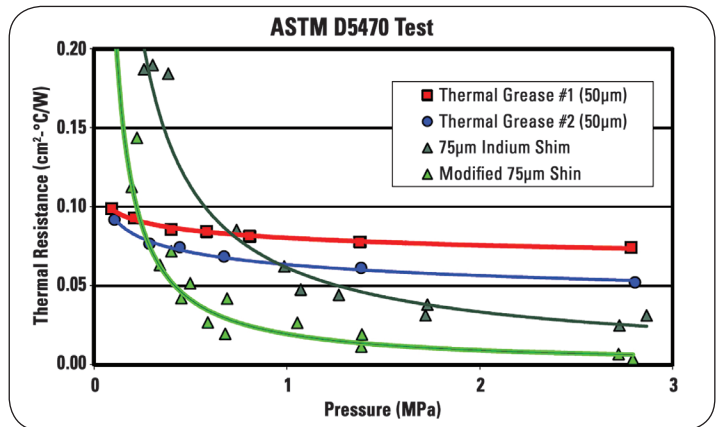


Figure 3. Plot of the thermal resistance of several TIM materials as a function of applied clamping pressure.

For greases, the wetting of the interface surfaces requires little force to achieve thermal contact. The application of clamping pressure reduces the interface resistance slightly by thinning the TIM.

In contrast, the metal TIM interface requires a clamping force of roughly half the yield point of the alloy to achieve the intimate contact needed for equivalent thermal resistance. The contact resistance continues to decrease asymptotically to the bondline thickness (BLT) limit as the pressure is increased further. The approach to the lower limit can be changed with modified processing. The lower line reflects this move toward lower resistance and faster approach to the limit.

The pressure response of the metal TIM of varying thicknesses is presented in Figures 4 and 5. The thermal resistance shows the predictable reduction with the bondline thickness for the thicker material. However, the trend is reversed for thin materials as the plastic flow is limited by the overlapping elastic stress fields at the contact points.

The resistance at the intercept (where  $P \rightarrow \infty$ ) is plotted in Figure 6. The linear relationship (with the exception of the thinnest foil) reflects the contribution of the bulk material conductivity to the thermal resistance. The slopes of the lines in Figure 5 reflect the interface resistance of the solid TIM in compression.

In contrast to the application of the ASTM D5470 test, the thermal test vehicle provides information at a single clamping pressure. However, it can provide a profile of the temperatures across the interface. This information provides insight into uniformity of the thermal resistance and the geometry of the degradation modes.

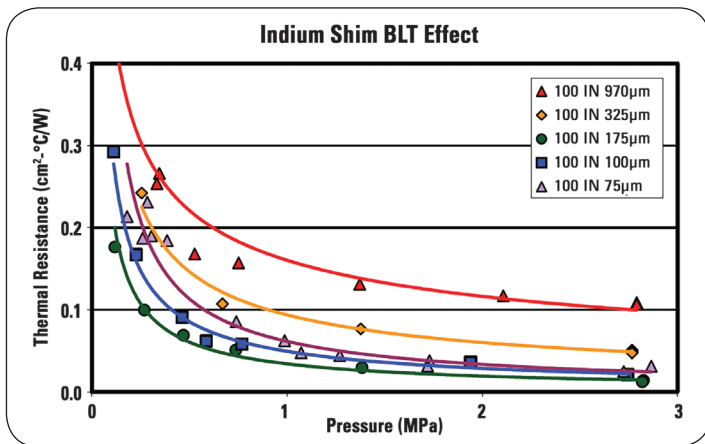


Figure 4. Plots of thermal resistance of indium shim of different thicknesses.

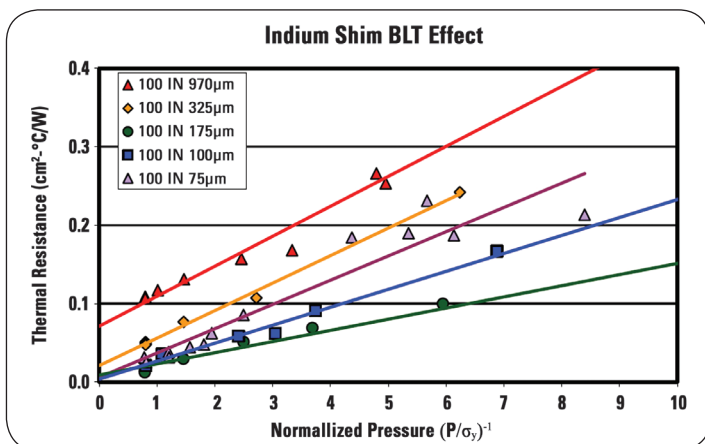


Figure 5. Plot showing the relationship thermal resistance vs. the inverse of pressure.

In Figures 7 and 8, the temperature profiles of common end-of-life failure modes of TIM materials are depicted in contrast to a stable TIM material. Figure 7 shows the profile of a TTV run through 1,000 power cycles from 0 to 50 watts. The flexing of the die due to the thermal expansion mismatch pumps grease out from the center of the TIM. A temperature

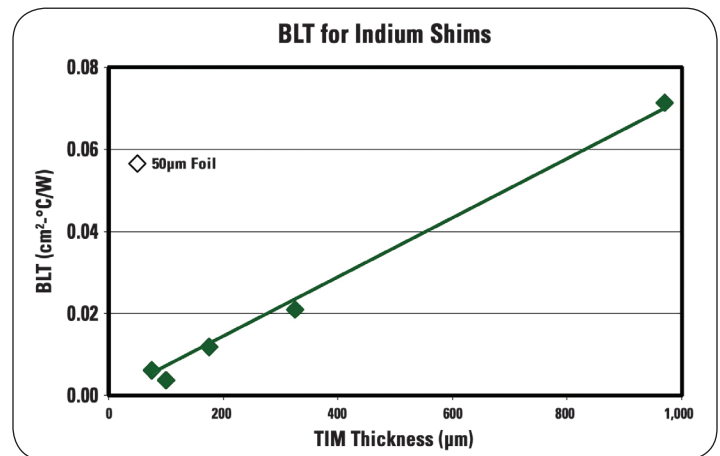


Figure 6. BLT thermal resistance contribution for the indium metal TIM.

peak in this area develops and grows with time.

In Figure 8, the same type of comparison is shown for the effect of drying of the grease during elevated temperature exposure. Again, the thermal resistance develops a temperature peak in the center of the die and degrades with time.

## Conclusion

In this paper, two steady state thermal testing methods are compared. The ASTM D5470 tester provides material behavior of materials at various temperatures and pressures. This provides application windows and comparative performance data for materials. The thermal test vehicle is specific to a single application but it can provide a wealth

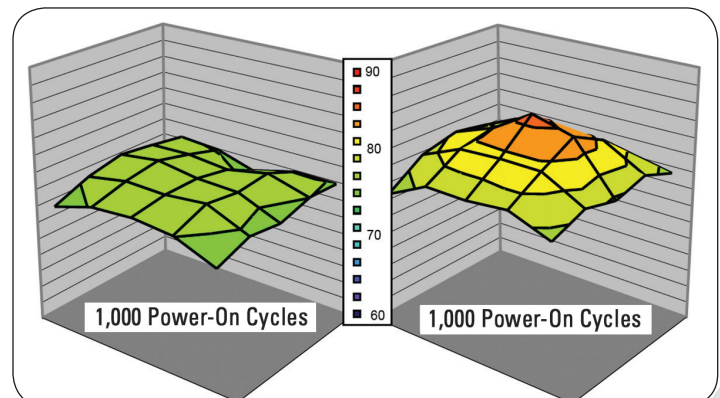


Figure 7. Temperature profiles of TIM materials subjected to power cycling. The thermal grease pump-out profile is shown on the right in contrast to a stable metal TIM on the left.

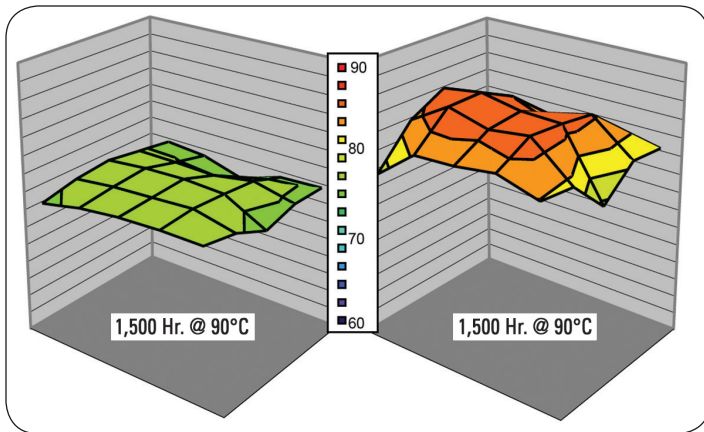


Figure 8. Temperature profiles of TIM materials after thermal exposure. The bake-out profile of grease is shown on the right in contrast to a stable metal TIM on the left.

of information about the performance of TIMs over their life cycles.

The combination of the two testing tools provides a more complete picture of a new TIM. This testing and understanding helps reduce risks associated with product introduction. Additionally, the performance measurements provide the information needed for intelligent product improvement.

## References

1. C. J. M. Lasance, C. T. Murray, D. L. Saums, M. Rencz, "Challenges in Thermal Interface Material Testing," Proc of 22th IEEE Semi-Therm Symposium, 2006.
2. ASTM: Standard Test Method for Thermal Transmission Properties of Thermally Conductive Electrical Insulation Materials, Designation D5470-06, ASTM International, 2006.
3. E. Samson, S. Machiroutu, J-Y. Chang, I. Santos, J. Hermerding, A. Dani, R. Prasher, D. W. Song. "Interface Material Selection and a Thermal Management Technique in Second Generation Platforms Built on Intel® Centrino™ Mobile Technology." Intel Technology Journal, vol. 09, Issue 01, February 2005.
4. G. Reza, "Accelerated Thermal and Mechanical Testing of CSP Assemblies," NASA JPL White Paper, <http://nepp.nasa.gov/docuploads/AFEF0D54-E6B6-49E3-AB978C0630AA6198/reza.pdf>, January 2001.
5. A. Poppe and V. Szekely, "Dynamic Temperature Measurements: Tools Providing a Look into Packaging and Mount Structures," Electronics Cooling, September 2000.
6. R. C. Campbell and S. E. Smith, "Flash Diffusivity Method: A Survey of Capabilities," Electronics Cooling, May 2002.
7. D. L. Saums, "ASTM D5470-06 Thermal Interface Material Test Stand," DS&A LLC, 2006.
8. B. N. Taylor and C. E. Kuyatt, NIST Technical Note 1297, "Guidelines for Evaluating and Expressing the Uncertainty of NIST Measurement Results," September 1994.

**First published at 23rd IEEE Semi-Therm Symposium,  
March 20–22, 2007, San Jose, California, USA.**